TECHNICAL MEMORANDUM

285

On the accuracy of the semi-geostrophic approximation

M.J.P. Cullen

Research Department

July 1999

European Centre for Medium-Range Weather Forecasts
Europäisches Zentrum für mittelfristige Wettervorhersage
Centre européen pour les prévisions météorologiques à moyen

Abstract

The semi-geostrophic model has been widely used to understand atmospheric flows such as fronts and developing cyclones. However, there have been a number of demonstrations of its lack of accuracy. This paper presents theory and computations to demonstrate that the semi-geostrophic model is an accurate approximation to the primitive equations on horizontal scales larger than the Rossby radius of deformation or when the ratio of horizontal to vertical scales is greater than f/N.

Keywords: Balance; Semi-geostrophic; Accuracy

1 Introduction

The semi-geostrophic approximation to the primitive equations was introduced by Eliassen (1947) and developed and popularised by Hoskins (1975). The semi-geostrophic equations have a very simple structure which allows solution by analytic techniques using the geostrophic coordinate transformation, and by geometrical techniques. Cullen *et al.* (1987) showd that the geometrical solution technique allows the equations to give understanding of a wide range of mesoscale phenomena, such as the limit on inland penetration of sea-breezes, barrier jets upstream of orography, and the control of convective mass transport by the large scale circulation.

Unfortunately, the semi-geostrophic model has been to some extent discredited by demonstrations of its lack of accuracy in solving problems where the primitive equations have smooth solutions and accurate comparison is possible. Examples include the comparison of solutions given by a set of different balanced models in Allen *et al.* (1990), and comparisons of baroclinic wave simulations by Snyder *et al.* (1991). The primitive equations in three dimensions have much more complex solutions than the shallow water equations, so in this context a highly accurate representation of the solution by a simple model is undesirable. However, estimates of accuracy are still needed to assess the usefulness of the predictions made by the simple models, in particular to assess in which asymptotic regimes the results are likely to be physically relevant.

The original assessment of accuracy by Hoskins (1975) was that for axisymmetric vortices, the worst case for the semi-geostrophic approximation, the error was 10 percent for cyclonic vortices with Rossby number 0.55 and anticyclonic vortices with Rossby number 0.2. These estimates are consistent with the more recent assessments of accuracy referred to above. In particular, the data used by Allen *et al.* contains strong anticyclonic vortices, which are shown to be the main source of error in the semi-geostrophic approximation.

In this paper we estimate the error by comparing the evolution of the potential vorticity with that of the equivalent potential vorticity derived from the primitive equations. Clearly a semi-geostrophic model cannot predict those parts of the primitive equation solution which are independent of the potential vorticity. To give a complete picture, we also compare the complete solution of the primitive equations with that derived by diagnosing the potential vorticity from the complete solution and inverting to obtain the dynamical

fields. This difference is a measure of the motions which are independent of the potential vorticity. For consistency, we carry out this procedure using the semi-geostrophic inversion procedure. The results show semi-geostrophic theory should be most accurate for length scales greater than the Rossby radius of deformation, or aspect ratios less than f/N. In this regime the potential vorticity is dominated by variations in static stability. We then demonstrate by computations with a shallow water model that the theoretical prediction that the error will be $O(Bu^2)$, where $Bu = Ro/Fr$, is observed in practice. We also compare the results with those given by a shallow water version of the nonlinear balance equation. The semi-geostrophic model has larger errors for $Bu = O(1)$, in agreement with the studies referred to above, but the errors become comparable for $Bu \leq 0.2$. We also show that the rate of transfer of energy to 'unbalanced' motions in the primitive equations is $O(Bu^2)$, given initial data in exact balance and using the semi-geostrophic definition of 'balance'.

The balance equations as used, for instance, in Holm (1996) and McWilliams *et. al.* (1999), are accurate for all Burger numbers. For ease of reference, we analyse the balance equations using the same methods as applied above to semi-geostrophic theory. The split between balanced and unbalanced parts of the solution to the primitive equations is now different, because the inversion procedure is different. The rate of generation of unbalanced energy from balanced initial data is also different. The evolution error of the potential vorticity is shown to be $O(Ro^3)$ or $O(Fr^2)$. However, the balance equations do not have such a simple solution structure, and spontaneous violations of the solvability conditions are possible. It remains to be demonstrated that they can give equivalent insights to those obtained by the semi-geostrophic model.

2 Approximation of Boussinesq incompressible flow by balanced systems

We use as 'exact' equations the non-hydrostatic, Boussinesq equations in Cartesian geometry, with constant Coriolis parameter f. These are sufficiently general to support the analyses carried out in this paper.

$$\begin{aligned} \frac{D\mathbf{v}}{Dt} + f\mathbf{k}\times\mathbf{v} + \nabla\phi &= g\theta\mathbf{k}/\theta_0 \\ \frac{D\theta}{Dt} &= 0 \\ \nabla.\mathbf{v} &= 0 \end{aligned} \tag{1}$$

The boundary conditions are that there is no normal flow at the rigid upper and lower boundaries $\delta\Gamma$ of a region Γ in (x, y, z), and there are periodic boundary conditions in x and y. Here z is a pseudo-height coordinate, as in Hoskins (1975), ϕ is the geopotential, and θ is the potential temperature, with basic state value θ_0. f and g are the Coriolis parameter and acceleration due to gravity. Energy conservation is expressed as

$$E = \int_\tau \{\frac{1}{2}(u^2 + v^2 + w^2) - g\theta z/\theta_0\} d\tau = \text{a constant} \tag{2}$$

These equations also conserve the Ertel potential vorticity

$$q = (\zeta + f).\nabla\theta \equiv (\nabla \times \mathbf{v} + f\hat{\mathbf{k}}).\nabla\theta \tag{3}$$

We will also illustrate the theory by using the shallow water form of the equations, using h as the depth of the fluid:

$$\begin{aligned} \frac{D\mathbf{v}}{Dt} + f\mathbf{k} \times \mathbf{v} + g\nabla h &= 0 \\ \frac{\partial h}{\partial t} + \nabla.h\mathbf{v} &= 0 \end{aligned} \tag{4}$$

Energy conservation is expressed as

$$E = \int_\tau \{\frac{1}{2}h(u^2 + v^2) + \frac{1}{2}gh^2\}d\tau = \text{a constant} \tag{5}$$

The potential vorticity is

$$q = \frac{(\zeta + f)}{h} \tag{6}$$

In either case, we can write the evolution equation for the potential vorticity as

$$\frac{\partial q}{\partial t} + \mathbf{u}.\nabla q = 0 \tag{7}$$

In order to assess how well the solutions of these equations can be approximated by those of a simpler model, we must define specific asymptotic regimes characterised by a small parameter. Assume horizontal and vertical length scales L and H, and velocity scale U. The Brunt-Vaisala frequency for equations (1) is $N^2 = g/\theta_0 \partial\theta/\partial z$. Then the Rossby number is defined by $Ro = U/fL$, the Froude number for equations (1) by $Fr = U/NH$, and for equations (4) by $Fr = U/\sqrt{(gh_0)}$, where h_0 is the mean value of h. The Burger number is defined as $Bu = Ro/Fr$. Note that only f, g, and h_0 are invariant in time. The other scaling parameters may change in magnitude during the flow evolution. In particular, Fr is quite robust for the shallow water equations, as it only varies with U, but is not robust for the three-dimensional equations where N and H can vary enormously in time.

We now assume that (1) or (4) is approximated by a balanced model which conserves potential vorticity. q is taken as the 'slow' variable , as in Vallis (1996). In the balanced model, the velocity, written as $\mathbf{u}_b$, can be derived from q by an invertibility relation (Hoskins et al. (1985)). Initialise both models with the same q. Then all the other fields required to solve the balanced model can be derived from q. The initial data for the exact equations is assumed to satisfy the scaling assumed for the asymptotic regime chosen, and these scale assumptions are assumed to remain valid in time. Then, if the asymptotic regime is characterised by a small parameter ϵ, we can estimate the error in evolution of the potential vorticity by seeking an estimate

$$\mathbf{u} = \mathbf{u}_b(1 + O(\epsilon^n)) \tag{8}$$

If this is satisfied, the evolution error in the potential vorticity will also be $O(\epsilon^n)$. Since the potential vorticity is assumed to be an unapproximated slow variable, the error in its

evolution is the important error to estimate in evaluating the accuracy of the balanced approximation. Another, separate, error measure is the accuracy to which a balanced state approximates the real state. One suitable measure of this is the difference bwtween the total energy E of the real state and the energy e of a balanced state having the same potential vorticity.

This type of analysis, though useful in understanding the behaviour of the atmosphere in different regimes, falls well short of a mathematically rigorous analysis, such as those carried out by Babin et al. (1996) and Embid and Majda (1996). A rigorous approach would be to initialise both sets of equations with the same values of all variables deribed by the invertibility principle from a given q. It would then be necessary to show that the solution of the exact equations diverged at a rate $O(\epsilon^n)$ from that of the balanced equations, with given values of f and g, but no constraints on horizontal or vertical scale other than those satisfied by the initial data. Such an analysis has to deal with the robustness of the asymptotic regimes. The ability of the exact equations to generate small scales very fast makes rigorous estimates difficult.

In order to understand how well the potential vorticity evolution is approximated, it is helpful to relate it to the other variables. This can be done using classical geostrophic adjustment theory which constructs a geostrophically balanced state with the same potential vorticity as the given data. If $Ro \ll Fr$ and $Bu \ll 1$, the underlying balanced state has approximately the same pressure and potential temperature field as the general state. We can also express this condition as $L \gg L_R$, where L_R is the Rossby radius of deformation. If $L \ll L_R$, so $Fr \ll 1, Bu \gg 1$, the underlying balanced state has approximately the same vertical component of vorticity as the general state but a different pressure and potential temperature field. This can be quantified using the theory of geostrophic adjustment for the linearised shallow water equations set out in Haltiner and Williams (1980). Consider the case where the pressure is a function of x only. The balanced state is given by

$$v_b = \frac{1}{1+(L_R/L)^2}\left((L_R/L)^2 v + i(fL)^{-1}h\right) \tag{9}$$
$$h_b = \frac{1}{1+(L_R/L)^2}\left(-i(L_R/L)^2 fLv + h\right)$$

(9) shows that

$$h_b = h(1 - O((L_R/L)^2)) + O((L_R/L)^2)h_v \tag{10}$$

where ϕ_v is the pressure field deduced by the inverse geostrophic relation from the wind field. In the large Burger number case

$$v_b = v(1 - O((L/L_R)^2)) + O((L/L_R)^2)v_g \tag{11}$$

We will generalise these estimates in the next sections.

3 Accuracy of the semi-geostrophic model

3.1 Formulation and method of analysis

The semi-geostrophic approximation to (1) takes the form

$$\begin{aligned} \frac{D\mathbf{v}_g}{Dt} + f\mathbf{k}\times\mathbf{v} + \nabla\phi &= 0 \\ \frac{D\theta}{Dt} &= 0 \\ (fv_g, -fu_g, g\theta\mathbf{k}/\theta_0) &= \nabla\phi \\ \nabla.\mathbf{v} &= 0 \end{aligned} \tag{12}$$

The third equation is a statement of the geostrophic and hydrostatic relations. These equations are valid for variable Coriolis parameter, but for the purposes of this paper we exploit the ability to analyse the equations in a simple way for the special case f constant. In that case we introduce the geostrophic and isentropic coordinates

$$(X, Y, Z) = (x + f^{-1}v_g, y - f^{-1}u_g, -g\theta/\theta_0) \tag{13}$$

We can then rewrite (12) as

$$\begin{aligned} \frac{D\mathbf{X}}{Dt} &= f^{-1}(u_g, v_g, 0) = -f^{-2}\mathbf{k}\times\nabla\phi \\ \mathbf{X} &= \nabla(\phi + \tfrac{1}{2}f^{-2}(x^2+y^2)) \\ \nabla.\mathbf{v} &= 0 \end{aligned} \tag{14}$$

We can interpret this equation as describing motion of particles in (X, Y, Z) space with a velocity $f^{-1}(u_g, v_g, 0)$. This can be shown to be non-divergent as a function of (X, Y, Z), so that the Jacobian

$$q = \frac{\partial(X, Y, Z)}{\partial(x, y, z)} \tag{15}$$

is conserved following the motion. This is the potential vorticity form of the equations introduced by Hoskins. Details of the derivation are given in Cullen and Purser (1989).

We now seek to estimate the accuracy of semi-geostrophic theory by comparing the evolution of q with that of an equivalent quantity derived from the primitive equations. We therefore need to project the solution of the primitive equations onto semi-geostrophic balanced states. First define

$$(X^*, Y^*, Z^*) = (x + f^{-1}v, y - f^{-1}u, -g\theta/\theta_0) \tag{16}$$

Then we can rewrite (1) as

$$\begin{aligned} \frac{D\mathbf{X}^*}{Dt} + f^{-2}\mathbf{k} \times \nabla\phi &= 0 \\ \frac{Dw}{Dt} + \frac{\partial\phi}{\partial z} &= g\theta/\theta_0 \\ \nabla.\mathbf{v} &= 0 \end{aligned} \tag{17}$$

Equations (17) conserve a potential vorticity

$$q^* = \frac{\partial(X^*, Y^*, Z^*)}{\partial(x, y, z)} \tag{18}$$

Given q^*, we can reconstruct the rest of the fields by first inverting (18) to give

$$\rho^* = \frac{\partial(x, y, z)}{\partial(X, Y, Z)} \tag{19}$$

This defines the volume of fluid which has specific values of $\mathbf{X}^*$. Then construct a state of the fluid satisfying

$$(X^*, Y^*, Z^*) = \nabla P \equiv \nabla(f^{-2}\phi^* + \frac{1}{2}f^{-2}(x^2 + y^2)) \tag{20}$$

with P convex, by carrying out a projection which moves fluid particles from positions $\mathbf{x}$ to new positions $\mathbf{x}^*$ in Γ while preserving their values of $\mathbf{X}^*$. Write this projection as

$$\begin{aligned} \Pi(u, v, w, \theta) &= (u_b, v_b, 0, \theta_b) \\ \mathbf{x}^* &= \mathbf{x} + (\xi, \eta, \zeta) \\ u_b(\mathbf{x}^*) &= u(\mathbf{x}) - \mathbf{f}\eta \\ v_b(\mathbf{x}^*) &= v(\mathbf{x}) + \mathbf{f}\xi \\ \theta_b(\mathbf{x}^*) &= \theta(\mathbf{x}) \end{aligned} \tag{21}$$

where the projection is generated by a displacement $\Xi = (\xi, \eta, \zeta)$ of the fluid which satisfies $\nabla.\Xi = 0$. The only boundary condition that can be specified is the statement

$$(x^*, y^*, z^*) \in \Gamma \tag{22}$$

which is ensured by setting $\Xi.\mathbf{n} = 0$ on $\partial\Gamma$. This is significantly different from the boundary conditions required in other forms of potential vorticity inversion. Shutts and Cullen (1987) show that this can be interpreted as minimising the energy integral

$$E = \int_\tau \{\frac{1}{2}(u^2 + v^2) - g\theta z/\theta_0\} d\tau \tag{23}$$

with respect to particle displacements that conserve $\mathbf{X}^*$.

For small departures from balance, the displacement can by estimated by a linearisation, scaled by a parameter α. Set

$$\begin{aligned} \nabla^2 p &= \nabla.(fv, -fu, -g\theta/\theta_0) \\ \frac{\partial p}{\partial n} &= (fv, -fu, -g\theta/\theta_0).\mathbf{n} \text{ on } \partial\Gamma \\ \Xi \equiv (\xi, \eta, \zeta) &= \alpha((fv, -fu, -g\theta/\theta_0) - \nabla\phi) \end{aligned} \tag{24}$$

The balanced state can be obtained by iteration of (24) with appropriate choices of α. Write the original, conserved, energy of the primitive equation solution as E, and the energy after minimisation as e^*. Then $(E - e^*)$ is a measure of the unbalanced energy, where balance is defined by semi-geostrophic theory. The change to the energy in one iteration is

$$\delta e = \alpha \int_\Gamma -f^2u^2 - f^2v^2 - (g\theta/\theta_0)^2 - (\nabla p)^2 d\tau \tag{25}$$

This is negative definite, and vanishes when the balanced state is reached. The relative changes to the wind and mass fields can be estimated by considering the effect on the two sides of the thermal wind equation; $f\frac{\partial v}{\partial z}$ and $\frac{g}{\theta_0}\frac{\partial \theta}{\partial x}$. The local change in v is approximately $(\frac{\partial v}{\partial x} + f\xi)$, and in θ is approximately $\zeta\frac{\partial \theta}{\partial z}$. Assuming ξ/ζ has magnitude L/H, the relative magnitude of the changes to the thermal wind balance is $1/Bu^2$. Thus the change to the pressure field in the low Burger number regime is $O(Bu^2)$ as given by the linear theory.

The magnitude of the displacement Ξ is determined by the amount by which the data fails to satisfy the geostrophic and hydrostatic relations themselves, which is O(Ro). If $L \gg L_R$, the projection primarily alters the velocity field. The correction required will be of order RoU, where U is the velocity scale, and the horizontal displacement required will thus be $\xi = O(RoU/f)$. Thus $\xi/L = O(Ro)^2$.

Note that, following Shutts and Cullen(1987), (25) can be used to deduce

$$\delta^2 e = \alpha \int_\Gamma \Xi.\Lambda.\Xi d\tau \tag{26}$$

where $\det\Lambda = q^*$, where Λ is the matrix with elements $\partial X_i/\partial x_j$. Thus we can estimate

$$E - e \leq \alpha \int_\Gamma \lambda |\Xi|^2 d\tau \tag{27}$$

where λ is the largest eigenvalue of Λ.

3.2 Accuracy of the evolution of potential vorticity

To estimate the error in the evolution implied by semi-geostrophic theory, assume that we have computed a solution of the primitive equations (17), with particle positions $\mathbf{x}(t)$, and particle values $\mathbf{X}^*(t)$. At each time t, we project to the balanced state using (21). This involves displacing the particles to new positions $\mathbf{x}^*(t)$ while preserving their values of X^*, Y^* and Z^*. Write $\frac{D^*}{Dt}$ to express a derivative following the 'minimum energy' particle positions $\mathbf{x}^*$, and write the 'velocity' that achieves this as $\mathbf{V} = (U, V, W)$. The condition

$\nabla.\Xi = 0$ implies $\nabla.\mathbf{V} = 0$. The boundary conditions (22) imply that $\mathbf{V}.\mathbf{n} = 0$ on $\partial\Gamma$. Then the equations expressing the evolution of this balanced state are

$$\begin{aligned} \frac{D^*\mathbf{X}^*}{Dt} + (f^{-2}\mathbf{k}\times\nabla\phi)^* &= 0 \\ \frac{D^*\alpha}{Dt} &= 0 \\ (X^*, Y^*, Z^*) &= \nabla P \end{aligned} \tag{28}$$

The * after the term in $\nabla\phi$ indicates that this term is calculated at $\mathbf{x(t)}$ from the solution of (17), and added to the solutions of (28) at positions $\mathbf{x}^*$. This means that (28) cannot be solved without prior knowledge of the solution of (17). However, (28) can be solved uniquely once $(\mathbf{k}\times\nabla\phi)^*$ is specified. The displacement means that $(\nabla\phi)^*$ is in general no longer the gradient of a scalar, and thus (28) does not conserve energy. Thus the balanced energy e^* can change in time. Note that this formulation is very close to the generalised Lagrangian mean form of equations introduced by Andrews and McIntyre (1978) and Buhler and McIntyre (1998) in the context of understanding wave-mean flow interaction.

Equations (28) represent the exact evolution of q^*, and are equivalent to the generic equation (7). The semi-geostrophic evolution of a state with the same potential vorticity can be obtained according to (12) by replacing the term $(\mathbf{k}\times\nabla\phi)^*$ in (28) with $\mathbf{k}\times\nabla\phi_b$, where $\phi_b = f^2(P - \frac{1}{2}(x^2+y^2)$ and P is the scalar potential appearing in (28).

Write

$$(\nabla\phi)^* = \nabla\phi - \xi.\nabla(\nabla\phi) + O(|\xi|^2) \tag{29}$$

Using $\nabla\phi = O(fU) + O(Ro)$, and the previous estimate $\xi = O(Ro^2L)$, the second term can be estimated as $Ro^2L.fU/L$. We can then say that

$$(\nabla\phi)^* - \nabla\phi_b = \nabla\phi(1 + O(Ro^2)) - \nabla\phi_b \tag{30}$$

As shown in the previous subsection, the difference $\nabla(\phi - \phi_b)$ can be estimated as $RoBu^2\nabla\phi_b$. Thus the overall error in the prediction of the balanced motion is $O(Ro^2)$, provided that $Bu^2 \leq Ro$. For a Rossby number of 0.1, this requires a Froude number of greater than 0.3. If this corresponds to a wind of $10ms^{-1}$ and a length scale of 1000km, this implies a vertical scale less than 3.3km for $N^2 = 10^{-2}$.

We can make a sharper estimate than (29) by time averaging the unbalanced motion. This procedure was used by Babin et al. (1997) and Embid and Majda (1996) in their analyses of the shallow water equations. This is only relevant if $Ro^2 > RoBu^2$. This estimate depends on the characterisation of the motion as a slowly varying pressure field, with particle positions changing as a result of both geostrophic motion and inertio-gravity oscillations superposed on the geostrophic motion. We first estimate the rate of change of the pressure field. Using the hydrostatic relation gives

$$\frac{\partial \phi}{\partial t} = \int \frac{g}{\theta_0}\frac{\partial \theta}{\partial t} \tag{31}$$

$$= \int \frac{g}{\theta_0}\mathbf{u}.\nabla\theta \simeq \frac{UH^2N^2}{L} \tag{32}$$

This estimate based on integrating the vertical pressure gradient is appropriate for the regime $L \gg L_R$. In contrast, the effective N^2 and Bu for the vertically meaned motion is infinite for incompressible flow. Since the geostrophic relation shows that $\phi \simeq LfU$, (31) shows that

$$\frac{\partial \phi}{\partial t} \simeq fBu^2\phi \tag{33}$$

The pressure tendency thus has a slower timescale than the inertial frequency by a factor Bu^2. Using the estimate $\nabla(\phi - \phi_b) \simeq RoBu^2\nabla\phi_b$, the same applies to the tendency of ϕ_b. Using (24), we have

$$f^2\xi = \frac{\partial \phi}{\partial x} - fv + O(\Xi.\nabla\frac{\partial \phi}{\partial x}) \tag{34}$$

$$f^2\eta = \frac{\partial \phi}{\partial y} + fu + O(\Xi.\nabla\frac{\partial \phi}{\partial y})$$

The vertical component ζ of the displacement is chosen to satisfy $\nabla.\Xi = 0$. Then we have from (17), writing a dot for a rate of change following particle positions

$$\ddot{x} + f^2\xi + O(\Xi.\nabla\frac{\partial \phi}{\partial x}) = 0 \tag{35}$$

$$\ddot{y} + f^2\eta + O(\Xi.\nabla\frac{\partial \phi}{\partial y} = 0$$

Use the definition $\mathbf{x}_c = \mathbf{x} + \Xi$, so that $\ddot{\mathbf{x}}_c = \ddot{\mathbf{x}} + \ddot{\Xi}$. This equation has two timescales f^{-1} and $(Bu^2f)^{-1} \equiv \tau^{-1}$. It is easy to see that it has solutions of the form

$$(\xi, \eta) = (\xi_0(\tau), \eta_0(\tau))e^{ift} \tag{36}$$

where

$$\ddot{x}_c + \dot{\eta}_0 \sin ft + O(\Xi.\nabla\frac{\partial \phi}{\partial x}) = 0 \tag{37}$$

$$\ddot{y}_c - \dot{\xi}_0 \sin ft + O(\Xi.\nabla\frac{\partial \phi}{\partial x}) = 0$$

All the terms in (37) are consistent with the slow time scale τ. Thus averaging over the period f^{-1} gives

$$\overline{\xi}^t = O(Bu^2)\xi = O((RoBu)^2L) \tag{38}$$

Taking the time mean of (29) thus improves the estimate of $(\nabla\phi)^* - \nabla\phi$ to $O((RoBu)^2)$. Since in this regime $Ro \ll 1$, the overall error estimate becomes $O(RoBu^2)$, as the term $\nabla(\phi - \phi_b)$ in (30) dominates. This is the prediction we test in our computations.

3.3 Rate of energy transfer between balanced and unbalanced flow

We first estimate the relative contributions to e of the kinetic and potential energy terms in (23). The available potential energy terms can be estimated from the difference between $\int g\theta z/\theta_0$ and the same quantity evaluated from a minimum energy configuration with θ a function of z only. This can be shown to give $(NH)^2\phi_b$, where ϕ_b measures the horizontally varying part of the pressure field. The kinetic energy density can be estimated using the geostrophic relation as $(fL)^{-2}\phi_b$ The kinetic energy is thus $O(Bu^2)e$.

The evolution of e can be calculated from (28). Replace $\mathbf{X}^*$ by the original variables, multiply the first equation by (u_b, v_b) and the second by z and add. Using $W = \frac{D^*z}{Dt}$, and the fact that $\mathbf{V}.\nabla s = -fUv_b + fVu_b - gW\theta/\theta_0$ integrates to zero, we find that

$$\frac{De}{Dt} = \int (u_b, v_b, 0).(\nabla\phi)^* \tag{39}$$

This is zero if $(\nabla\phi)^*$ can be written as $\nabla\pi$ for some scalar π, because $\nabla.(u_b, v_b, 0) = 0$. In general, (30) gives $(\nabla\phi)^* = \nabla\phi(1 + O(Ro^2))$. In the time mean, the difference will be improved to $O((RoBu)^2)$. Thus we have

$$\frac{De}{Dt} = O(f(RoBu)^2)\int (u_b^2 + v_b^2) = O(f(RoBu)^2Bu^2)e \tag{40}$$

This suggests that energy will only transfer between the balanced and unbalanced flow on a timescale $\tau(RoBu)^{-2}$. Thus in well initialised computations, the rate of generation of unbalanced energy should be $O(RoBu)^2$. We test this in our computations also.

Now calculate the value of $E - e$ which is consistent with the scaling. Allowing for the relative dominance of the potential energy in the balanced state, and the dominance of the velocity perturbation in the unbalanced component, this gives $E - e = O((RoBu)^2)E$. Equation (40) shows that $E - e$ varies over a time scale τ^{-1}, which is the 'slow' timescale for equation (35). The overall picture is thus self-consistent.

Using (29), we can also seek a sharper estimate by calculating the condition that $(\nabla\phi)^* = \nabla\pi$ to leading order in Ξ. This gives

$$\frac{\partial\xi}{\partial y}\frac{\partial^2 p}{\partial x^2} + \frac{\partial\eta}{\partial y}\frac{\partial^2 p}{\partial x\partial y} - \frac{\partial\xi}{\partial x}\frac{\partial^2 p}{\partial y\partial x} - \frac{\partial\eta}{\partial x}\frac{\partial^2 p}{\partial y^2} = 0 \tag{41}$$

This is satisfied for flows independent of one horizontal coordinate. This fits with the original semi-geostrophic scaling of Hoskins and Bretherton (1972), which permits L to be arbitarily small in one direction as long as it stays large in the other. The energy estimate shows that a genuinely two-dimensional flow will conserve its balanced energy, and thus the partition of energy between balanced and unbalanced motion is fixed for all time.

It will be of interest to seek other cases where (41) is either zero, or smaller than would be expected from general estimates. In such cases $\frac{\partial e}{\partial t}$ will be small, and if $E - e$ is initially small, it will only grow slowly, so that the flow stays closer to balance than would normally be expected.

The accuracy estimates above agree with the standard asymptotic error estimate, showing that the latter is consistent. This is because the terms neglected in semi-geostrophic theory are $\frac{Du_{ag}}{Dt}$. Since $u_{ag} = O(Ro)u_g$ and $\frac{D}{Dt} = O(Ro)f$, the neglected terms are $O(Ro)^2$ smaller than the largest retained terms.

4 Accuracy of the balance equations

4.1 Formulation and method of analysis

We summarise the accuracy estimates for the balance equations using a similar framework to that set out above for semi-geostrophic theory. This helps to relate the behaviour of the two models. Vallis (1996) also presents analyses of various forms of the balance equation based on potential vorticity.

Write the decomposition of the velocity field into rotational and divergent parts as

$$\begin{aligned} \mathbf{u} = &\ (u_r, v_r, 0) + (u_d, v_d, w) \\ \nabla_h.(u_r, v_r, 0) = &\ 0 \\ \nabla_h \times (u_d, v_d, 0) = &\ 0 \end{aligned} \tag{42}$$

Since $\nabla.\mathbf{u}_d = 0$, w is the only independent variable in $\mathbf{u}_d$, with u_d and v_d determined from it. Following Holm (1996), we write the Hamiltonian form of the balance equations as

$$\begin{aligned} \frac{D}{Dt}(u_r, v_r) + (u_r \nabla_h u_d + v_r \nabla_h v_d) + (-fv, fu) + \nabla_h \phi = 0 \\ \frac{D\theta}{Dt} = 0 \\ \frac{\partial \phi}{\partial z} - g\theta/\theta_0 + \mathbf{u}_r \cdot \frac{\partial \mathbf{u}_d}{\partial z} \end{aligned} \tag{43}$$

These equations conserve energy (with only the rotational wind appearing in the kinetic energy) and potential vorticity

$$q_{BE} = (\nabla \times \mathbf{v}_r + f\hat{\mathbf{k}}).\nabla\theta \tag{44}$$

$\mathbf{u}_d$ is determined implicitly. If q_{BE} is given, $\mathbf{v}_r$ and θ can be calculated by using the diagnostic relation obtained from taking the horizontal divergence of (43). $\mathbf{u}_d$ can be determined implicitly from the time derivative of this relation. Write these calculations in the form

$$(\mathbf{v}_r, \mathbf{v}_d, \theta) = B(q_{BE}) \tag{45}$$

Then a natural projection from the solutions of the primitive equations (1) to those of (43) is to set

$$\Pi_{BE}(\mathbf{v}, \theta) = B(q) \tag{46}$$

4.2 Accuracy of the evolution of potential vorticity

If equations (1) and (43) are started with the same potential vorticity, the error in evolution will simply be the error in the advecting velocity, since both models conserve potential vorticity. Holm (1996) (eq. (5.10)) shows that taking the horizontal divergence and vertical derivative of the momentum equation in (43) gives an omega equation of the form

$$-S(z)\nabla^2 w - f^2\frac{\partial^2 w}{\partial z^2} + \text{LOT} = 0 \tag{47}$$

where $S(z)$ is of order N^2, and LOT denotes terms of lower order in derivatives of w. The largest terms in LOT will typically be $\nabla^2(\mathbf{v}_r \cdot \nabla\theta)$ and $f\partial/\partial z(\nabla\mathbf{v}_r \cdot \nabla\mathbf{v}_r)$. These have magnitudes s HN^2U/L^3 and $fU^2/(HL^2)$. The ratio of these terms is $Ro : Fr^2$. The coefficients of w in (43) have magnitudes N^2/L^2 and f^2/H^2, with ratio $Ro^2 : Fr^2$. Thus for $Bu \ll 1$, we have $w \simeq RoUH/L$, and for $Bu \gg 1$, $w \simeq UH/L$.

If we derive an equation of the form (47) directly from (1), we obtain

$$\frac{\partial^2}{\partial t^2}\frac{\partial^2 w}{\partial z^2} - S(z)\nabla^2 w - f^2\frac{\partial^2 w}{\partial z^2} + \text{LOT} = 0 \tag{48}$$

If the solution of (47) is substituted directly into (48), and we asume that the time variations in LOT are on an advective timescale U/L, then the error in w resulting from using (47) is $O(Fr^2)$ if $Bu \gg 1$ and $O(Ro^2)$ if $Bu \ll 1$. Thus the error in the evolution of q will be respectively $O(Fr^2)$ and $O(Ro^3)$. For $Bu = 1$ the error is $O(Ro^2) = O(Fr^2)$. We will demonstrate the improvement for $Bu \ll 1$ in our computations.

In general, (48) has fast wave solutions which will grow as a result of the time-dependence of LOT even if absent from the initial data. The asymptotic analysis of Ford *et al.* (1999) shows that their growth is at $O(Fr^2)$, but their interaction back on the potential vorticity, which only depends on the time-averaged effect of the waves, is at $O(Fr^4)$. Applying the same argument for $Bu \ll 1$ shows that the rate of growth of inertio-gravity wave energy will be $O(Ro^3)$. Embid and Majda (1996) and Babin *et al.* (1996,1997) carry out rigorous analyses of this effect using time averaging over the fast waves.

5 Computational tests

5.1 Numerical models used

The experiments are designed to test the predictions that the errors in semi-geostrophic theory scale as $O(Bu^2)$ for fixed Ro, and the rate of generation of unbalanced energy from initialised data is also $O(Bu^2)$. We use a set of spherical shallow water models. The semi-geostrophic model is that described and used by Mawson (1996). It uses semi-lagrangian advection of the primitive variables (u_g, v_g, h), and an implicit method of calculating (u, v) to ensure that the geostrophic relation is satisfied at each new time level. The variables

(h, u, v) are held on a C grid, and (u_g, v_g) are held on a D grid. The implicit equations are solved by a multigrid method. The data are initialised by first choosing analytic height and geostrophic wind fields, and then carrying out the discrete initialisation procedure set out in Mawson (1996). The initial values of u and v are set by making an initial time step, and calculating the u and v needed to preserve geostrophic balance.

The primitive equation model is a shallow water version of the implicit version of the UK Meteorological Office model (Cullen et al. (1997)). It uses a C grid, semi-lagrangian advection, and multigrid solution of the implicit equations. The nonlinear balance equations are solved by adapting the primitive equation code. Equation (47) in shallow water form becomes

$$gh_0\nabla^2\nabla\cdot v - f^2\nabla\cdot v + \mathrm{LOT} = 0 \tag{49}$$

This is used to calculate the divergence at each timestep, and then the condition $v_d^{t+\delta t} = v_d^t$ is enforced by correcting $\mathbf{v}_r$ and h iteratively while conserving the potential vorticity. This can be achieved by setting

$$\begin{aligned} gh_0\nabla^2 D - f^2\nabla D &= v_d^{(n)t+\delta t} - v_d^{(n)t} \\ \nabla\cdot(U,V) &= D \\ h^{(n+1)} &= h^{(n)} - h_0 D \\ u^{(n+1)} &= u^{(n)} + fV \\ v^{(n+1)} &= v^{(n)} - fU \end{aligned} \tag{50}$$

D is a correction with the same dimensions as a divergence.

The initial values are set by carrying out a short initial timestep and performing the necessary iterative solution.

5.2 Experiment design

The initial data are chosen to give a wavenumber 2 pattern in each hemisphere, with no height perturbation close to the equator (Fig.1). This is legal initial data for the semi-geostrophic model, which has to have inertially stable data. The data are initialised for the semi-geostrophic model, and then passed to the primitive equation model. Both models are run for 2 days. The results from the primitive equation model are then initialised using the semi-geostrophic initialisation procedure, and compared with the semi-geostrophic results. This gives the evolution error of the semi-geostrophic model. The unbalanced energy in the primitive equation model is estimated from the difference made by initialising the day 2 results. The procedure is shown diagrammatically in Fig.2. The evolution error is $B - V$, and the unbalanced part of the primitive equation solutions is $P - V$.

The same design is used to measure the error of the nonlinear balanced model. The initialised data used in the first experiment is re-initialised using the nonlinear balance model. The primitive and nonlinear balanced models are run for 2 days, and the results

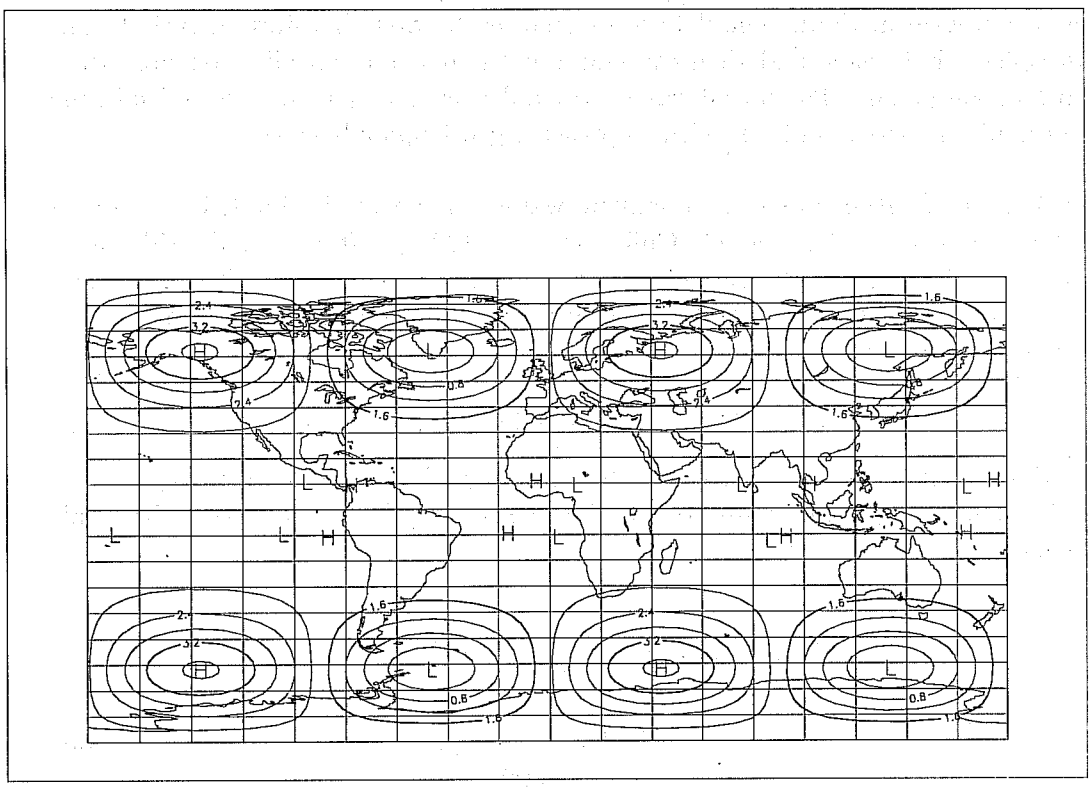

Figure 1: Initial height data for shallow water tests

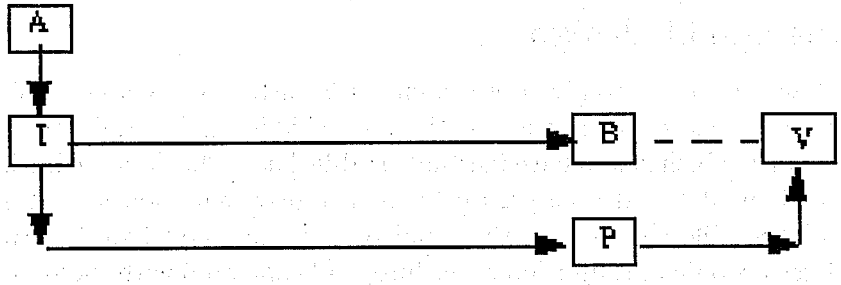

Figure 2: Experimental setup: A-analytic initial data, I-data initialised for balanced model, B-forecast using balanced model, P-forecast using primitive equation model, V-initialised end state from primitive equation model

compared as above. Since the two initialisation procedures are different, the two primitive equation runs are also slightly different.

The base resolution for the experiments was a latitude longitude grid with 96 points around latitude circles and 65 points between the poles. The results were also generated using a higher resolution of 192x129 points. Though the general behaviour as the parameters were varied was the same for both resolutions, in the semi-geostrophic tests there were significant differences in individual results. The complete semi-geostrophic experiment was thus also run at the higher resolution, and a further check carried out using a 288x193 grid for one set of parameters. The nonlinear balance model is more compatible with the primitive equation model. Sample runs with the 192x129 grid showed that it was unnecessary to repeat the whole experiment at higher resolution.

The experiments were designed to test the effect of varying Burger number for fixed Rossby number. Thus the same perturbation height field was used for all runs, but the mean value was varied from 5760m down to 182.5m. The amplitude of the superposed wave was $\pm 170m$, so that the lowest mean value used is just sufficient to avoid the height becoming zero. The horizontal velocity had a maximum value of about $10ms^{-1}$. the gravity wave speed associated with the mean height varied from $240ms^{-1}$ to $42ms^{-1}$. Table 1 lists the values used, together with typical Froude and Burger numbers.

Table 1: Parameters used.

ϕ_0 m	$Ro = U/fL$	$Fr = U/\sqrt{(g\phi_0)}$
5760	0.04	0.04
2880	0.04	0.06
1440	0.04	0.08
720	0.04	0.11
360	0.04	0.16
180	0.04	0.22

5.3 Results

The results for the height evolution errors are shown in Fig.3, with the wind errors in Fig.4. The results for the measures of imbalance are shown in Figs 5 and 6. The experiment was carried out as above with one exception. It proved impossible to initialise the day 2 results from the primitive equation model at high resolution and large values of the mean height using the semi-geostrophic initialisation scheme., which was based on a local iteration. This was because of the development of significant height perturbations at the equator, and the availability of only a local iteration to remove negative potential vorticity, as described in Mawson (1996). A different, non-local, initialisation algorithm would be required to resolve this problem. The two parts of the error are therefore plotted together in the relevant parts of Figs.3 to 6. Results for individual cases run at higher resolution are also plotted to validate the results.

It is readily seen that the $O(Bu^2)$ behaviour expected for the evolution error of the semi-geostrophic model is clearly demonstrated. The behaviour of the nonlinear balanced model is consistent with an $O(Bu)$ behaviour of the error for $Bu \ll 1$. The much lower errors for the balanced model for larger values of mean height is consistent with the results of Allen et al. (1990). The two models have comparable errors once the gravity wave speed is of the order of $50ms^{-1}$.

The measures of imbalance also show the expected behaviour. In the semi-geostrophic case the $O(Bu^2)$ behaviour is clearly seen at high resolution, though the low resolution results are less reliable in this measure. In the balance equation results, the rate of generation of gravity wave energy clearly reduces for small Bu.

6 Conclusions

We have demonstrated the expected rate of convergence for small Burger number in the semi-geostrophic model, and shown that the errors are comparable to those of the nonlinear balance equation in the small Burger number regime. This should help to formalise the applicability of the wide range of analytic and geometric predictions that can be made using semi-geostrophic theory. We note that neither model shows greater accuracy in predicting the potential vorticity than in predicting the total evolution. The imbalance errors and potential vorticity evolution errors are of comparable size for all cases tested. The results would have to be averaged over the inertio-gravity wave period before we could expect to demonstrate higher accuracy in potential vorticity evolution. This is difficult in a real case such as that illustrated because of the wide range of inertio-gravity wave frequencies present.

References

Allen, J. S., Barth, J. A. and Newberger, P. 1990 On intermediate models for barotropic continental shelf and slope flow fields. Part III: Comparison of numerical model solutions in periodic channels. *J. Phys. Oceanog.*, **20,** 1949-1973

Andrews, D. G. and McIntyre, M. E. 1978 An exact theory of nonlinear waves on a Lagrangian mean flow. *J. Fluid Mech.*, **89,** 609-646

Babin, A., Mahalov, A. and Nicolaenko, B. 1996 Global splitting, integrability and regularity of 3D Euler and Navier-Stokes equations for uniformly rotating fluids. *Eur. J. Mech.,B/Fluids*, **15,** 291-300

Babin, A., Mahalov, A. and Nicolaenko, B. 1997 Regularity and integrability of rotating shallow water equations. *C.R.Acad.Sci. Paris*, **324,** 593-598

Buhler, O. and McIntyre, M. E. 1998 On non-dissipative wave-mean interactions in the atmosphere or oceans. *J. Fluid Mech.* , **354,** 301-343

Cullen, M. J. P., Norbury, J., Purser, R. J. and Shutts, G. J. 1987 Modelling the quasi-equilibrium dynamics of the atmosphere. *Quart. J. Roy. Meteor. Soc.*, **113,** 735-757

Cullen, M. J. P. and Purser, R. J. 1989 Properties of the Lagrangian semi-geostrophic equations. *J. Atmos. Sci.*, **46**, 2684-2697

Cullen, M. J. P., Davies, T., Mawson, M. H., James, J. A. and Coulter, S. 1997 An overview of numerical methods for the next generation UK NWP and climate model. in 'Numerical Methods in Atmosphere and Ocean Modelling', The Andre Robert Memorial Volume. (C.Lin, R.Laprise, H.Ritchie, Eds.), Canadian Meteorological and Oceanographic Society, Ottawa, Canada, 425-444

Eliassen, A. 1948 The quasi-static equations of motion. *Geofys. Publ.*, **17**, no.3

Embid, P. F. and Majda, A. J. 1996 Averaging over fast waves for geophysical flows with arbitrary potential vorticity. *Comm. Partial Diff. Eqs.*, **21**, 619-658

Ford, R., McIntyre, M. E. and Norton, W. A. 1999 Balance and the slow quasi-manifold: some explicit results. *J. Atmos. Sci.*, **56**, xxx-xxx

Haltiner, G. J. and Williams, R. T. 1980 *Numerical prediction and Dynamic Meteorology*, 2nd ed. Jchn Wiley and Sons. 477pp.

Holm, D. D. 1996 Hamiltonian balance equations. *Physica D* , **98**, 379-414

Hoskins, B. J. 1975 The geostrophic momentum approximation and the semigeostrophic equations. *J. Atmos. Sci.*, **32**, 233-242

Hoskins, B. J. and Bretherton, F. P. 1999 Atmospheric frontogenesis models: Mathematical formulation and solution. *J. Atmos. Sci.*, **29**, 11-37

Hoskins, B. J., McIntyre, M. E. and Robertson, A. W. 1985 On the use and signifance of isentropic potential vorticity maps. *Quart. J. Roy. Meteor. Soc.*, **111**, 887-946

McWilliams, J. C., Yavneh, I., Cullen, M. J. P. and Gent, P. R. 1999 The breakdown of large-scale flows in rotating, stratified fluids. *Phys. Fluids* , **xx**, xxx-xxx

Shutts, G. J. and Cullen, M. J. P. 1987 Parcel stability and its relation to semigeostrophic theory. *J. Atmos. Sci.*, **46**, 2684-2697

Snyder, C., Skamarock, W. C. and Rotunno, R. 1991 A comparison of primitive-equation and semi-geostrophic simulations of baroclinic waves. *J. Atmos. Sci.*, **48**, 2179-2194

Vallis, G. K. 1996 Mechanisms and parametrizations of geostrophic adjustment and a variational approach to balanced flow. *Quart. J. Roy. Meteor. Soc.* , **122**, 291-322

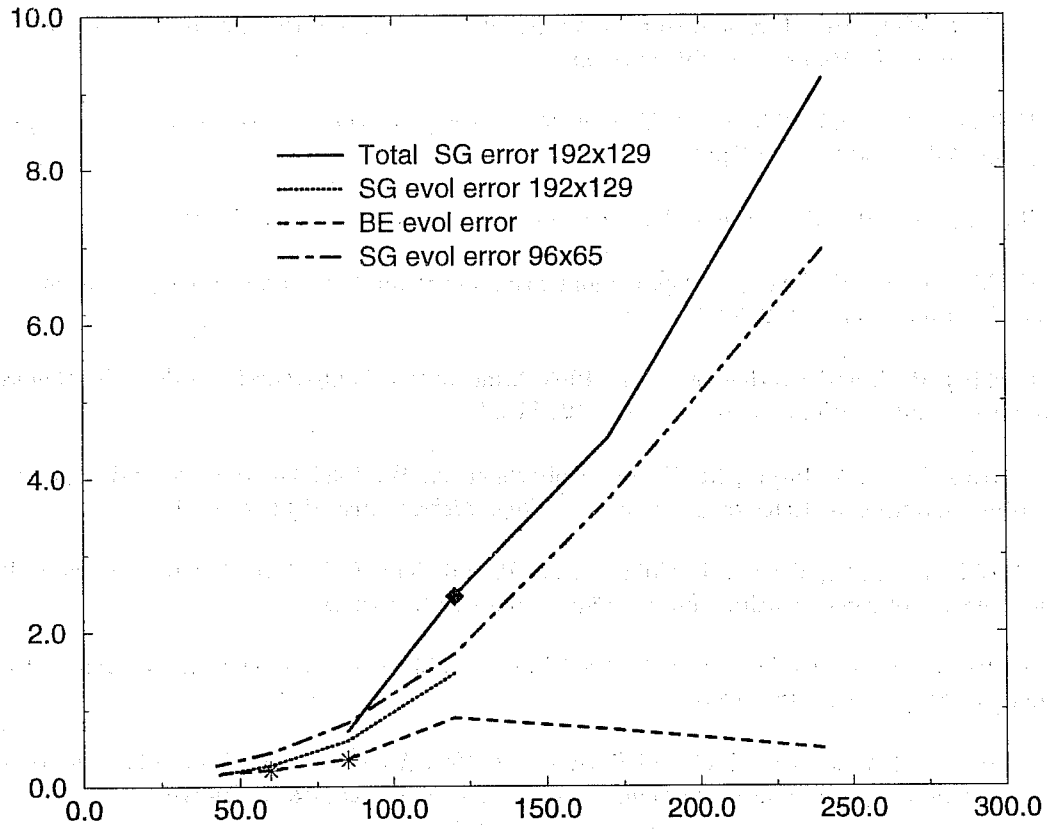

Figure 3: r.m.s. height evolution errors (m) after 48 hours plotted against gravity wave speed (ms^{-1}). Stars indicate balance equation results on a 192x129 grid, the diamond a semi-geostrophic result on a 288x193 grid.

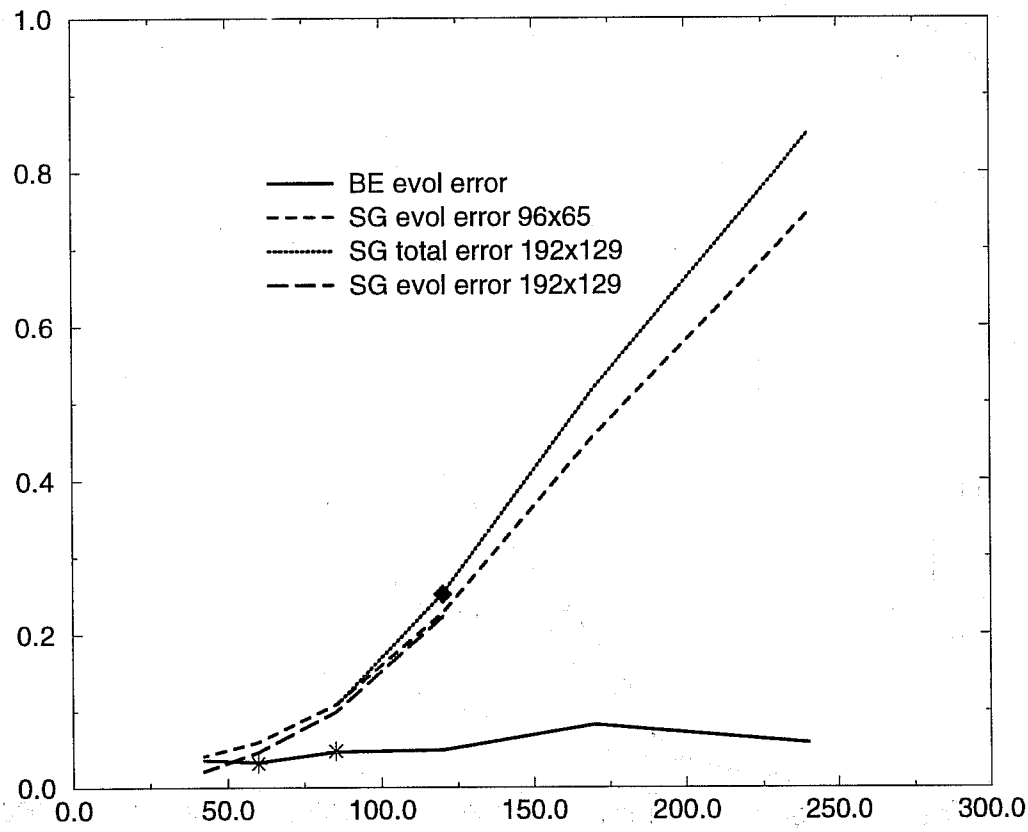

Figure 4: r.m.s. wind evolution errors (ms^{-1})) after 48 hours plotted against gravity wave speed (ms^{-1}). Notation as Fig.3

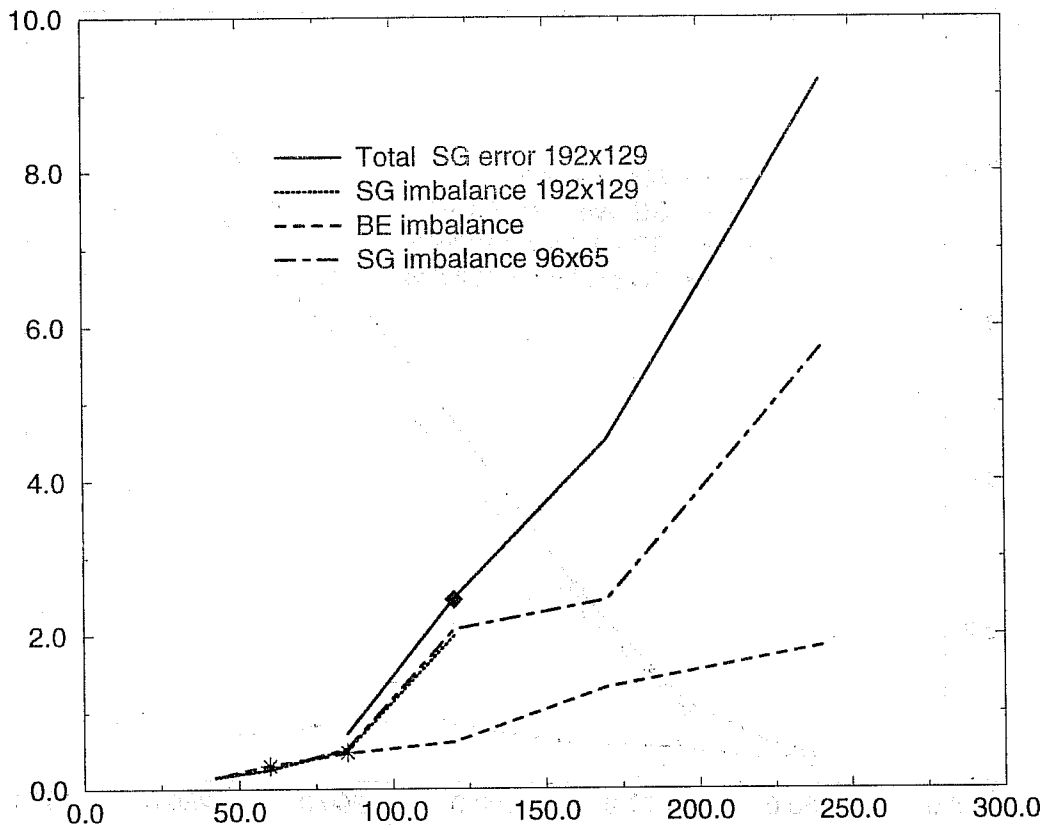

Figure 5: r.m.s. height imbalances (m) after 48 hours plotted against gravity wave speed (ms^{-1}). Notation as Fig.3

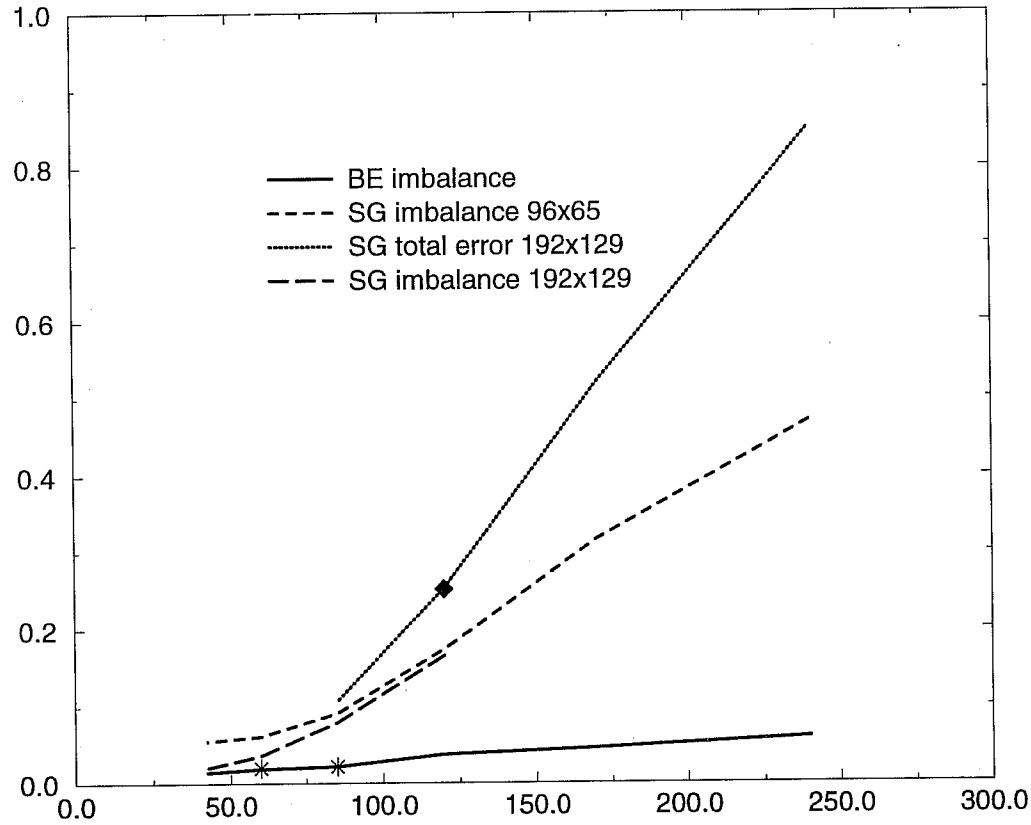

Figure 6: r.m.s. wind imbalances (ms^{-1}) after 48 hours plotted against gravity wave speed (ms^{-1}). Notation as Fig.3